jmb Communication

Conformational Selection in Substrate Recognition by Hsp70 Chaperones

Moritz Marcinowski[1,2], Mathias Rosam[1,2], Christine Seitz[2,3], Johannes Elferich[2,3], Julia Behnke[1,2], Claudia Bello[1,2], Matthias J. Feige[1,2], Christian F. W. Becker[1,2], Iris Antes[2,3] and Johannes Buchner[1,2]

*1 - **Department Chemie,** Technische Universität München, 85748 Garching, Germany*
*2 - **Center for Integrated Protein Science Munich,** Munich, Germany*
*3 - **Department Biowissenschaftliche Grundlagen,** Technische Universität München, 85354 Freising, Germany*

***Correspondence to Iris Antes and Johannes Buchner:** I. Antes is to be contacted at Wissenschaftszentrum Weihenstephan, Technische Universität München, Emil-Erlenmeyer-Forum 8, 85354 Freising, Germany; J. Buchner, Department Chemie, Technische Universität München, Lichtenbergstraße 4, 85748 Garching, Germany. antes@wzw.tum.de; johannes.buchner@tum.de*
http://dx.doi.org/10.1016/j.jmb.2012.11.030
Edited by S. Radford

Abstract

Hsp70s are molecular chaperones involved in the folding and assembly of proteins. They recognize hydrophobic amino acid stretches in their substrate binding groove. However, a detailed understanding of substrate specificity is still missing. Here, we use the endoplasmic reticulum-resident Hsp70 BiP to identify binding sites in a natural client protein. Two sites are mutually recognized and form stable Hsp70–substrate complexes. *In silico* and *in vitro* analyses revealed an extended substrate conformation as a crucial factor for interaction and show an unexpected plasticity of the substrate binding groove. The basic binding mechanism is conserved among different Hsp70s.

Introduction

Molecular chaperones share the remarkable ability to bind and release nonnative proteins.[1] One of the major chaperone classes is the ATP-dependent Hsp70 family. Hsp70s consist of an N-terminal nucleotide binding domain connected by a flexible linker to a C-terminal substrate binding domain (SBD).[2–4] Exposed stretches of hydrophobic residues were recognized as a signature of Hsp70 substrates.[5,6] Based on these studies, a scoring algorithm was developed to classify and identify binding peptides.[5,7–10] However, differences in substrate recognition exist between Hsp70s[11–13] and our current understanding is not sufficient to predict binding sequences.[8]

With a view to define key elements of substrate recognition, we determined the binding sites in an endogenous substrate for BiP, the Hsp70 orthologue of the endoplasmic reticulum (ER).[6,14–16] The interaction of BiP with substrate proteins can be transient[17,18] but stable complexes with certain substrates are also observed,[19,20] especially for antibody heavy chains (HCs) that are retained in the ER, if not assembled with a light chain.[21–23] In fact, it has been shown that HCs do not even cycle from BiP *in vivo*[20] where a multichaperone complex is involved in antibody biogenesis.[24] This quality control mechanism is based on an unfolded C_H1 domain in the HC that only folds upon interaction with the light chain.[25–27]

So far, binding sequences in C_H1 were only identified via stimulation of BiP's ATPase activity by C_H1-derived peptides.[28] However, this approach cannot report on their recognition within the full-length domain and it does not assess the stability of the BiP–peptide complexes.[29]

Here, we show that the conformation of substrate peptides plays a pivotal role in the binding process.

Identification of BiP binding sites within an authentic substrate protein

Like all Hsp70 members, the molecular chaperone BiP recognizes stretches of several amino acids in

nonnative proteins.[30,31] The antibody C_H1 domain is an important substrate of BiP,[21,22] allowing the retention of unpaired HCs in the ER.[20,25–27] Authentic BiP binding sites are generally unknown. In the C_H1 domain, they were only analyzed by the ability of C_H1-specific peptides to stimulate BiP's ATPase activity.[28]

For a direct anisotropy-based binding assay, predicted C_H1-derived binding peptides were labeled with a fluorophore.[32] Only two of the five C_H1-derived peptides that stimulated BiP's ATPase activity to the largest extent,[28] SVFPLAP and HTFPAVL, bound to BiP with low micromolar affinities (K_d = 12.5 μM and 11.1 μM, respectively; Fig. 1a, Ref. 32 and Table 1). Single point mutations rendered these into non-binding variants (HTFAAVL and SVKPLAP; Fig. 1b and Fig. S1). Importantly, if separately introduced into the full-length domain, these mutations also decreased the affinity of BiP for C_H1 (from K_d = 12.9 μM for C_H1 wild type (wt) to K_d = 14.8 μM for C_H1 HTFAAVL and to K_d = 25.1 μM for C_H1 SVKPLAP; Fig. 1c and Table 1). The respective C_H1 double mutant abolished BiP

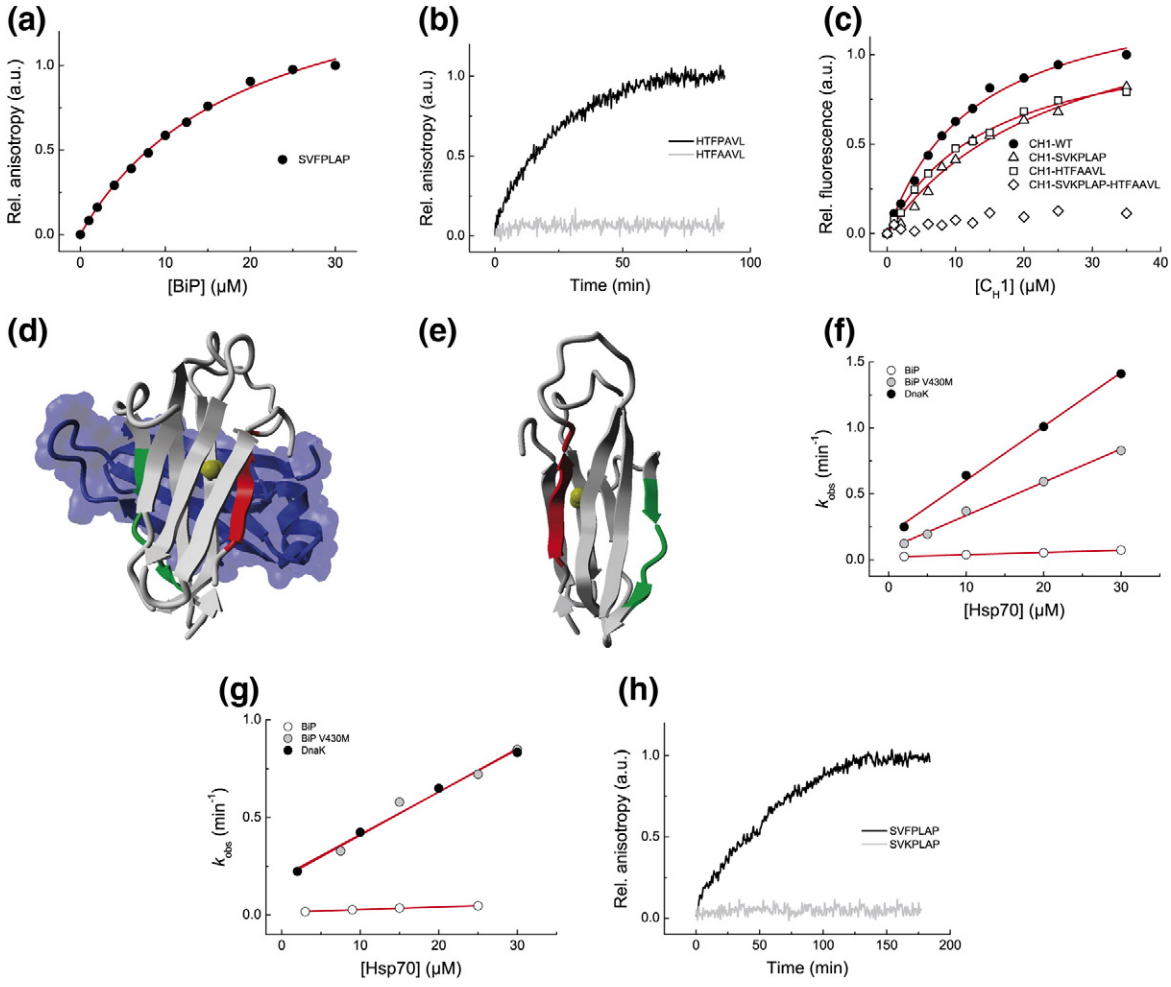

Fig. 1. Substrate binding by BiP wt, BiP V430M, and DnaK and location of the BiP binding sites in C_H1. (a and b) Binding of lucifer yellow-labeled peptides was analyzed by fluorescence anisotropy. (a) The K_d of BiP and the SVFPLAP peptide was determined as K_d = 19.3 ± 1.4 μM. (b) Analysis of the HTFAAVL peptide association with 15 μM BiP in the presence of 1 mM ADP (gray trace) in comparison to the HTFPAVL wt peptide (black trace). (c) Complex formation of the C_H1 domain with BiP was analyzed in SEC-HPLC experiments for 1 μM BiP and varying C_H1 concentrations in the presence of 1 mM ADP. For the wt, data were fit to a K_d of 12.9 ± 1.1 μM. For the SVKPLAP mutant, a K_d of 25.1 ± 4.2 μM was obtained, and for the HTFAAVL mutant, the K_d was 14.8 ± 1.1 μM. The binding analysis of the C_H1 double mutant SVKPLAP–HTFAAVL to BiP did not result in any complex formation. (d and e) BiP binding sequences in human IgG1 C_H1 are highlighted in red (SVFPLAP) and green (HTFPAVL) on the structure of C_H1 (gray) in complex with C_L (blue) (d) and on the isolated C_H1 domain (e). The internal disulfide bridge of C_H1 is shown as yellow balls (PDB ID: 1HZH). (f and g) Rate constants for binding of 1 μM labeled SVFPLAP (f) or HTFPAVL peptide (g) to varying concentrations of BiP wt, BiP V430M, and DnaK were determined and plotted against Hsp70 concentration to derive k_{on} and k_{off}. Data for BiP binding to the HTFPAVL peptide in (g) were adapted from Ref. 32. Note that the DnaK data partly hide the BiP V430M data in (g). (h) BiP binding of the SVKPLAP peptide (gray trace) in comparison to the SVFPLAP wt peptide (black trace) under identical conditions as in (b).

Table 1. k_{on}, k_{off}, and K_d for substrate binding by BiP and DnaK

Substrate	Hsp70	k_{on} (μM^{-1} min^{-1})	k_{off} (min^{-1})	K_d (μM)	Source
SVFPLAP	BiP	0.0017 ± 0.0001	0.0213 ± 0.0013	12.5[a] 19.3 ± 1.4[b]	Fig. 1a and f
	BiP V430M	0.0252 ± 0.0010	0.0834 ± 0.0171	3.3[a]	Fig. 1f
	DnaK	0.0409 ± 0.0016	0.1944 ± 0.0292	4.8[a]	Fig. 1f
HTFPAVL	BiP	0.0013 ± 0.0001[c]	0.0144 ± 0.0012[c]	11.1[a] 11.6 ± 0.6[b,c]	Ref. 32
	BiP V430M	0.0222 ± 0.0017	0.1869 ± 0.0320	8.4[a]	Fig. 1g
	DnaK	0.0218 ± 0.0010	0.1956 ± 0.0195	9.0[a]	Fig. 1g
C_H1 wt	BiP	n.d.	n.d.	12.9 ± 1.1[b]	Fig. 1c
C_H1 SVKPLAP	BiP	n.d.	n.d.	25.1 ± 4.2[b]	Fig. 1c
C_H1 HTFAAVL	BiP	n.d.	n.d.	14.8 ± 1.1[b]	Fig. 1c
C_H1 SVKPLAP-HTFPAVL	BiP	n.d.	n.d.	Not determinable	Fig. 1c

n.d., not determined.

k_{on} and k_{off} (± standard errors) were determined from linear fits of the observed rate constants k_{obs} from Figs. 1 and 2 for BiP wt, BiP V430M, and DnaK with the peptides SVFPLAP and HTFPAVL. The K_d values were calculated and experimentally determined for BiP. The K_d values for BiP and the C_H1 variants were determined by SEC-HPLC experiments as detailed in Materials and methods.

[a] Calculated K_d values.

[b] Experimentally determined K_d values.

[c] Adapted from Ref. 32.

binding completely (Fig. 1c). This indicates that these two sequences are critical for BiP binding to C_H1, which might contribute to the high stability of BiP–HC complexes observed *in vivo*.[20]

Interestingly, only one BiP molecule can bind to C_H1 at a time.[32] SVFPLAP and HTFPAVL are found in regions that form β-strands in the folded structure of C_H1 and are located in the C_H1–C_L interface of the fully assembled antibody (Fig. 1d and e).[33] The decrease in affinity upon mutation of either site shows that both can be recognized. Their localization in the interface is also in agreement with the competition of BiP and C_L for binding.[25] This explains the absence of triple BiP–C_H1–C_L complexes during antibody assembly as the C_H1 residues that interact with BiP or C_L overlap.[25] Importantly, both sequences are highly conserved in IgG (Fig. S2).

Current models of peptide binding to BiP are based on the peptide's hydrophobicity[7,28] and cannot explain the non-binding behavior of HTFAAVL as exchanging Pro against Ala does not lead to a substantial change in hydrophobicity. Thus, an additional factor besides hydrophobicity seems to influence BiP binding.

Comparison of substrate binding by BiP and DnaK

To follow up on the unexpected behavior of the HTFAAVL mutation, we investigated peptide binding to BiP and DnaK, an *Escherichia coli* Hsp70, in detail (Fig. 1 and Table 1).

For the wt peptide HTFPAVL, BiP showed a k_{on} of 0.0013 μM^{-1} min^{-1} and a k_{off} of 0.0144 min^{-1}, resulting in a K_d of 11.1 μM (Fig. 1g and Table 1, Ref. 32). The peptide SVFPLAP resulted in a k_{on} of 0.0017 μM^{-1} min^{-1} and a k_{off} of 0.0213 min^{-1} with a calculated K_d of 12.5 μM similar to the equilibrium value (Fig. 1f and Table 1).

However, DnaK associated up to ~24-fold faster with the peptides than BiP (k_{on} = 0.0409 μM^{-1} min^{-1} and 0.0218 μM^{-1} min^{-1} for SVFPLAP and HTFPAVL, respectively; Figs. 1f and g and 2d; Table 1) and the DnaK–peptide complexes were kinetically less stable as the k_{off} rates were also up to ~14-fold higher (Fig. 2d and Table 1). This resulted in calculated K_d values for DnaK in the same range as those for BiP with K_d = 4.8 μM and 9.0 μM for SVFPLAP and HTFPAVL, respectively (Table 1).

We also analyzed binding of the nonnative peptides SVKPLAP and HTFAAVL, which abolished binding to BiP (Fig. 1h and b). DnaK showed significantly reduced affinity for the mutant SVKPLAP peptide and no binding to the HTFAAVL peptide (Fig. S1 and Fig. 3b). Interestingly, DnaK was also able to bind the C_H1 wt domain yet not the C_H1 double mutant (Fig. S3a and b). Taken together, DnaK bound the same sequences with similar affinities as BiP, yet with different kinetics in agreement with previous studies.[11]

Structural basis of peptide binding

To investigate the structural aspects of peptide binding to BiP and DnaK, we performed molecular dynamics and docking simulations of the peptides in complex with DnaK [Protein Data Bank (PDB) ID: 1DKX[30]] and a homology model of BiP's SBD, which is based on the above structure of DnaK, using the program DynaDock[34] (see SI Methods and Results). The docking protocol allowed forward and backward binding, but very few energetically favorable backward conformations were obtained and none of them was among the energetically best conformations. Computationally, both the *cis* and *trans* Pro connections were investigated.

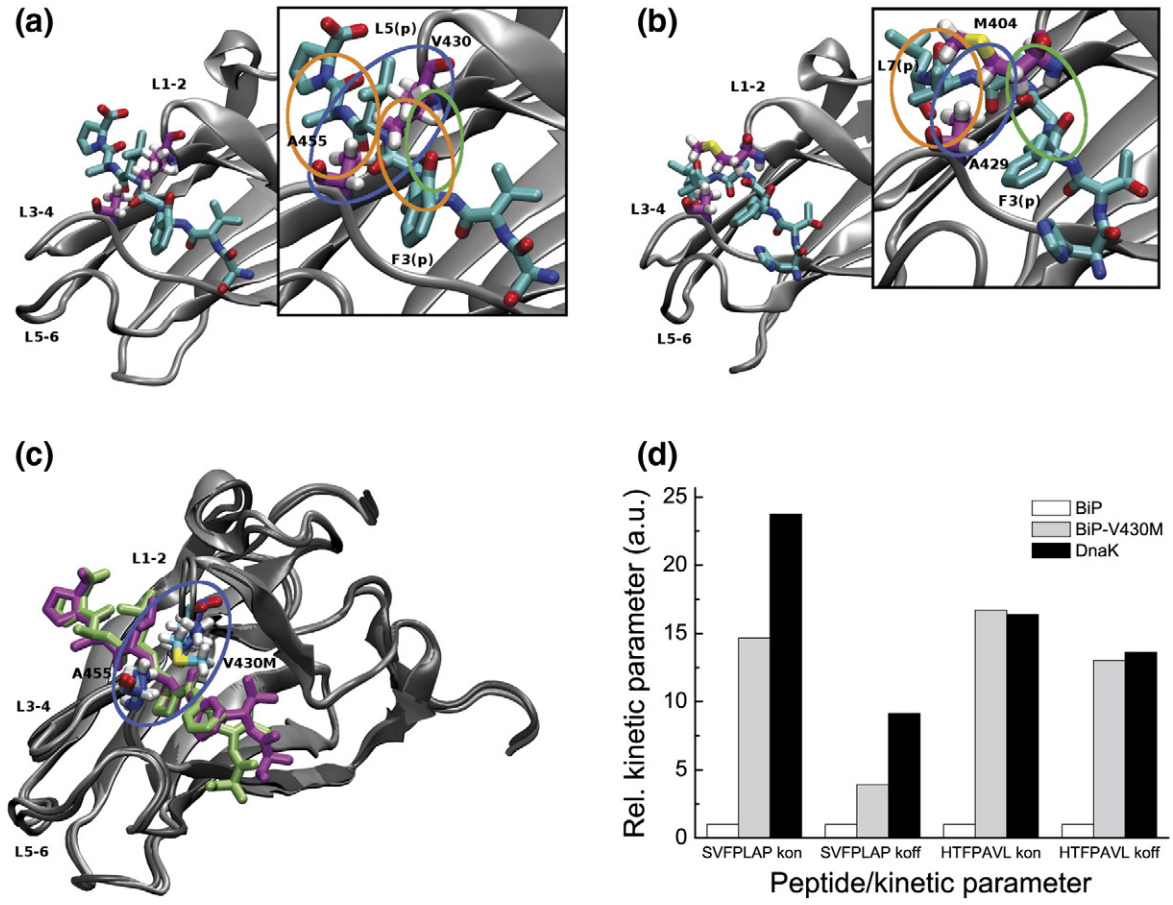

Fig. 2. Structures of DnaK and BiP in their bound state and analysis of the BiP V430M mutant. (a) BiP binding site with the bound SVFPLAP peptide and (b) DnaK binding site with bound HTFPAVL peptide. Bridging residues are shown in magenta and the bound peptide is shown in licorice representation. The hydrophobic bridge is surrounded by a blue circle, the protein–peptide backbone hydrogen bond is surrounded by a green circle, and the hydrophobic protein–peptide side-chain interactions are surrounded by orange circles. (c) Superposed structures of the best-scoring docking poses of SVFPLAP in the BiP wt (protein, silver cartoon; peptide, magenta licorice; bridging residues, blue licorice) and V430M mutant (protein, black cartoon; peptide, lime licorice; bridging residues, cyan licorice) binding sites, respectively. (d) Comparison of BiP wt, BiP V430M, and DnaK with respect to their substrate peptide association and dissociation rates determined by fluorescence anisotropy. The data sets were normalized to BiP wt.

Our simulations revealed two important factors for stable peptide binding: (i) the complementarity of the binding sites' central hydrophobic pocket with the fourth peptide residue (p4) and (ii) the stable bridging conformation of the loops L1–2 and L3–4 in a closed state above the peptide, which is consistent with the literature, at least for DnaK[35] (Fig. 2). This bridge was stabilized by a backbone hydrogen bond between the peptide and residue V430 in BiP (M404 in DnaK) and hydrophobic interactions between p3 and p5 and residues within the loops L1–2 and L3–4 (Fig. 2a and b). These features correlated with the structural stability of the complexes (Table S1). The two wt peptides HTFPAVL and SVFPLAP show all of these features in BiP complexes (Fig. 2a and b). For HTFAAVL, the P4A mutation led to a strong destabilization of the complex due to an overall instable binding of A4 in the central binding pocket. This eventually leads to bridge opening above the peptide (Fig. S4a). In addition, we calculated the binding free-energy change upon mutation to HTFAAVL using the linear interaction energy approximation (see SI) and obtained a $\Delta\Delta G$ of 44.50 kcal mol^{-1}.

Analysis of the peptide complexes with DnaK led to similar results (Table S1). However, the hydrophobic bridge above the bound peptide was less stable. Interestingly, BiP differs from DnaK only in a single amino acid (V430M) in these loops. Simulations showed that this residue was critical for the closing of the bridge, which is more stable in BiP (Fig. 2b and c).

When we experimentally analyzed the binding kinetics of the wt peptides to the respective BiP V430M mutant, we observed an ~15-fold (SVFPLAP) and an ~17-fold (HTFPAVL) acceleration of the k_{on}

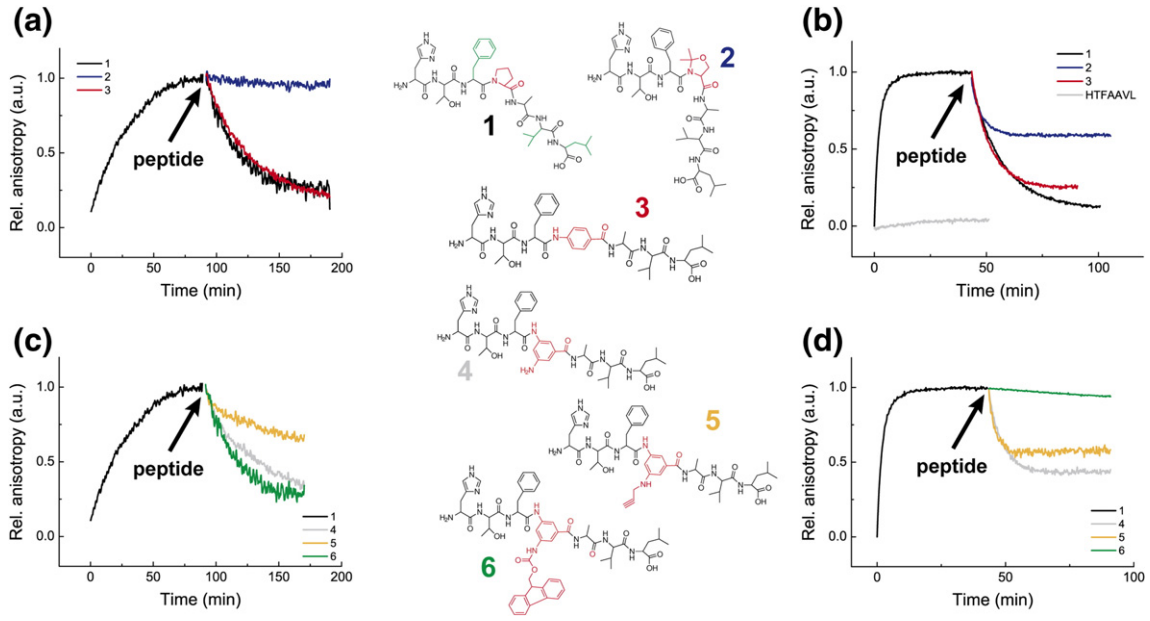

Fig. 3. Hsp70 binding of peptides containing non-proteinogenic amino acids. Analysis was performed by competition experiments of preformed complexes of 1 μM lucifer yellow-labeled wt peptide HTFPAVL (1) and Hsp70 in the presence of 1 mM ADP and was followed by fluorescence anisotropy. Dissociation was induced by addition of a 150-fold excess of unlabeled peptide over the labeled peptide. The central Pro residue was exchanged against 5-dimethyl-4-oxaproline (2) or 4-aminobenzoic acid (3). (a) Dissociation of preformed BiP–peptide complexes (15 μM) by a 150-fold excess of peptide 2 (blue trace), peptide 3 (red trace), and the wt peptide 1 (black trace, adapted from Ref. 32). (b) Dissociation of preformed DnaK–peptide (10 μM) complexes by a 150-fold excess of peptide 2 (blue trace), peptide 3 (red trace), and the wt peptide 1 (black trace). The binding of 1 μM HTFAAVL peptide is shown in gray. The central Pro residue was exchanged against 1,3-diaminobenzoic acid (4) or propargyl-substituted 1,3-diaminobenzoic acid (5) and Fmoc-substituted 1,3-diaminobenzoic acid (6) to test for the influence of varying side-chain lengths. (c) Dissociation of preformed BiP–peptide complexes (15 μM) by a 150-fold excess of peptide 4 (gray trace), peptide 5 (orange trace), and peptide 6 (green trace). (d) Dissociation of preformed DnaK–peptide (10 μM) complexes by a 150-fold excess of peptide 4 (gray trace), peptide 5 (orange trace), and peptide 6 (green trace).

values (Figs. 1f and g and 2d; Table 1). Similarly, also the k_{off} rates were accelerated ~4-fold (SVFPLAP) and ~13-fold (HTFPAVL), clearly shifting BiP's affinities towards the DnaK values (Figs. 1f and g and 2d; Table 1). Thus, we could transfer binding characteristics from DnaK to BiP by a single point mutation in the bridge, identifying this region as important for fine-tuning the interaction of different Hsp70s with substrates.

Structural analyses of the peptide binding modes in the publicly available experimental structures of DnaK–peptide complexes support the above binding pattern together with the extended peptide conformation, which can also be found in all experimental structures. This confirms the importance of these concepts for Hsp70–peptide binding in general.[30,36–39]

Effects of peptide conformation on Hsp70 interaction

The binding-abolishing P4A mutation in HTFPAVL and our docking results suggest that not only the peptide's hydrophobicity but also the peptide's specific binding interactions and potentially its conformations are important for stable binding. Hence, we integrated non-proteinogenic amino acids to stabilize specific conformations. As shown in Fig. 3a (1–3), the central Pro of HTFPAVL (1) was exchanged against 5-dimethyl-4-oxaproline (2) to stabilize a kinked conformation and 4-aminobenzoic acid (3) to stabilize an extended conformation. We tested the ability of these peptides to dissociate preformed complexes of BiP with the fluorescently labeled HTFPAVL peptide. For the kinked peptide 2, no decay in the fluorescence anisotropy of the bound wt peptide was observable (Fig. 3a). In contrast, peptide 3 dissociated the complex efficiently (Fig. 3a). These results demonstrate that peptide conformation has a substantial impact on complex formation with elongated conformations being highly favored over kinked ones. In the case of the bacterial DnaK, the kinked peptide 2 dissociated the DnaK–HTFPAVL complex less efficiently than the elongated peptide 3, which exhibited almost wt-like displacement efficiency (Fig. 3b).

To test the binding pocket flexibility, we exchanged p4 against 1,3-diaminobenzoic acid, which allowed

further modification with either a propargyl or Fmoc substituent (Fig. 3, peptides 4, 5, and 6, respectively). Surprisingly, while the small propargyl substituent resulted in decreased binding to BiP, the peptide modified with the large Fmoc group dissociated the wt peptide as well as the peptide containing unmodified 1,3-diaminobenzoic acid (Fig. 3c). For DnaK, the Fmoc substituent did not dissociate the wt peptide while both other peptides dissociated the complex to a certain extent (Fig. 3d). These results indicate that Hsp70s differ in accommodating modified side chains in their binding pockets.

Docking of peptides 2 to 6 into BiP and DnaK led to increased distances of the bridging residues and only rare formation of the protein–peptide backbone hydrogen bond (Table S1). However, in most cases, the bridge was stabilized by additional interactions with the non-proteinogenic amino acid leading to stable binding (Fig. S4). In agreement with our experiments, similar peptide binding behavior was observed for BiP and DnaK, except for peptides 2 and 6 (Fig. S5). The latter is caused by differences in the plasticity of the BiP and DnaK binding sites: DnaK adapted to peptide 2 such that bridge formation was possible, whereas BiP could not (Fig. S5a and b). On the other hand, BiP formed stable complexes with peptide 6 with the large Fmoc group fitting well inside the binding pocket, whereas in DnaK, the Fmoc group could not enter the site (Fig. S5c and d). This indicates significant differences in the dynamics of the SBDs as the pockets' sequences are 100% conserved between BiP and DnaK.

The structural features of the binding sites for Hsp70 chaperones are still poorly understood. It is known that short stretches of amino acids are bound and that hydrophobic side chains are important for the formation of stable complexes.[5,7,8,10,28,40] In this work, we show directly that substrate conformation also plays an important role in the recognition process.

Importantly, for a mutation that changed the conformation and abolished binding (HTFPAVL to HTFAAVL), the hydrophobicity and the prediction of the BiP scoring algorithm[28] were not altered while this was the case for the SVKPLAP mutant.

Due to its rigidity, the central Pro leads to a defined and stable conformation of its neighbor residues. This might explain the stronger binding of HTFPAVL compared to HTFAAVL, in which the combination of the two central small and flexible Ala residues leads to an overall increased peptide flexibility and thus destabilization of a stretched conformation with p4 located inside the central binding pocket. In agreement with this notion, peptides containing amino acid analogs with constraint ring structures bind efficiently to Hsp70s. In contrast, the stabilization of a kinked conformation by introducing 5-dimethyl-4-oxaproline reduced binding to BiP strongly. These observations suggest the preferred binding of peptides in an extended conformation by Hsp70s.

In general, the hydrophobicity of Hsp70 binding sequences seems to have co-evolved with an extended conformation of the respective amino acid stretches. In agreement with this notion, most known Hsp70 binding sites are located in β-sheet regions and thus occur in an extended conformation. This concept is modulated by flexibility differences in the binding clefts of BiP and DnaK, which allows accommodation of various side-chain geometries as shown for non-natural amino acids.

Thus, efficient binding of a peptide to an Hsp70 member induces (i) an extended conformation of the peptide, which allows aligning with the binding pocket, and (ii) an induced-fit-like docking of the p4 side chain into the central binding pocket. These processes are followed by (iii) the closing of the loops L1–2 and L3–4 over the binding pocket for the formation of kinetically stable complexes.

Materials and methods

Protein production

BiP and DnaK were purified as described previously.[32,41] Expression, purification, and refolding of the oxidized human IgG1 C_H1 domain were performed as described previously.[25] The C_H1 mutants were generated via site-directed mutagenesis and purified as the wt.

Analytical SEC-HPLC experiments

Size-exclusion chromatography (SEC)-HPLC experiments were performed as described previously to determine C_H1 binding to BiP at 37 °C in the presence of 1 mM ADP in HKM buffer (50 mM Hepes–KOH, pH 7.5, 150 mM KCl, and 10 mM $MgCl_2$).[25]

Peptides

The wt and the SVKPLAPGSC and HTFAAVLGSC peptides were purchased (Biomatik, USA). All non-proteinogenic peptides were synthesized by solid phase peptide synthesis[42] following the *in situ* neutralization protocol for Boc-chemistry[43] or standard Fmoc-deprotection procedures and HBTU-activated couplings[44] (SI methods). Peptide labeling was performed as described previously.[32]

Fluorescence spectroscopy

Fluorescence measurements were carried out as described previously.[32] Briefly, analyses were performed in a 1-cm quartz cuvette in a Spex FluoroMaxIII spectrofluorimeter with anisotropy polarizers (Jobin Yvon, Germany). Lucifer yellow-labeled HTFPAVLGSC peptide (1 μM) and varying concentrations of Hsp70 were used in HKM buffer with 1 mM ADP. Lucifer yellow was excited at 430 nm and fluorescence was detected at 525 nm. Rate

constants and K_d values were obtained by single exponential fits assuming a single binding site.

Homology modeling and docking

Docking calculations were performed using DynaDock[34] and a Modeller-created[45,46] homology model for BiP based on DnaK's structure (PDB ID: 1DKX[30]). Re- and cross-docking evaluation runs were performed with DynaDock for two experimental DnaK–peptide complexes (PDB IDs: 1DKX[30] and 3DPO[36] and an NMR structure of apo-DnaK[37]). Details of the modeling procedures are provided in the SI.

Acknowledgements

We thank Ruoyu Sun for help with protein purification and measurements, Katja Baeuml for assistance with peptide synthesis and purification, and Martin Haslbeck for the DnaK proteins. We gratefully acknowledge funding provided by the Studienstiftung des deutschen Volkes (to M.M.), the German Academy of Sciences Leopoldina (grant number LPDS 2009-32 to M.J.F.), the Humboldt Foundation (to C.B.), and the Deutsche Forschungsgemeinschaft, the Fonds der Chemischen Industrie, and the Bayerische Forschungsstiftung (to J.B.). I.A. was supported by CIPSM Women.

Author Contributions. M.M. and M.R. purified proteins and performed experiments. C.S. and J.E. performed molecular docking and simulation. J.Be. and C.B. synthesized peptides. M.M., M.R., M.J.F., C.F.W.B., I.A., and J.B. designed experiments, evaluated data, and wrote the manuscript.

Conflict of Interest. The authors declare that they have no conflict of interest.

Supplementary Data

Supplementary data to this article can be found online at http://dx.doi.org/10.1016/j.jmb.2012.11.030

Received 29 August 2012;
Received in revised form 23 November 2012;
Accepted 26 November 2012
Available online 1 December 2012

Keywords:
antibody;
BiP;
Hsp70;
molecular chaperone;
substrate conformation

Present addresses: M. Marcinowski, Roche Diagnostics GmbH, 82377 Penzberg, Germany; J. Behnke, Department of Genetics and Tumor Cell Biology, St. Jude Children's Research Hospital, Memphis, TN 38105-3678, USA; C. Bello, Institut für Biologische Chemie, Fakultät Chemie, Universität Wien, 1090 Wien, Austria; M. J. Feige, Department of Genetics and Tumor Cell Biology, St. Jude Children's Research Hospital, Memphis, TN 38105-3678, USA; C. F. W. Becker, Institut für Biologische Chemie, Fakultät Chemie, Universität Wien, 1090 Wien, Austria.

Abbreviations used:
SBD, substrate binding domain; ER, endoplasmic reticulum; HC, heavy chain; wt, wild type; PDB, Protein Data Bank; SEC, size-exclusion chromatography.

References

1. Mayer, M. P. (2010). Gymnastics of molecular chaperones. *Mol. Cell*, **39**, 321–331.
2. Goloubinoff, P. & De Los Rios, P. (2007). The mechanism of Hsp70 chaperones: (entropic) pulling the models together. *Trends Biochem. Sci.* **32**, 372–380.
3. Swain, J. F., Dinler, G., Sivendran, R., Montgomery, D. L., Stotz, M. & Gierasch, L. M. (2007). Hsp70 chaperone ligands control domain association via an allosteric mechanism mediated by the interdomain linker. *Mol. Cell*, **26**, 27–39.
4. Takeda, S. & McKay, D. B. (1996). Kinetics of peptide binding to the bovine 70 kDa heat shock cognate protein, a molecular chaperone. *Biochemistry*, **35**, 4636–4644.
5. Gething, M. J., Blond-Elguindi, S., Buchner, J., Fourie, A., Knarr, G., Modrow, S. *et al.* (1995). Binding sites for Hsp70 molecular chaperones in natural proteins. *Cold Spring Harbor Symp. Quant. Biol.* **60**, 417–428.
6. Karlin, S. & Brocchieri, L. (1998). Heat shock protein 70 family: multiple sequence comparisons, function, and evolution. *J. Mol. Evol.* **47**, 565–577.
7. Blond-Elguindi, S., Cwirla, S. E., Dower, W. J., Lipshutz, R. J., Sprang, S. R., Sambrook, J. F. & Gething, M. J. (1993). Affinity panning of a library of peptides displayed on bacteriophages reveals the binding specificity of BiP. *Cell*, **75**, 717–728.
8. Knarr, G., Modrow, S., Todd, A., Gething, M. J. & Buchner, J. (1999). BiP-binding sequences in HIV gp160. Implications for the binding specificity of bip. *J. Biol. Chem.* **274**, 29850–29857.
9. Pandya, M. J., Bendz, H., Manzenrieder, F., Noessner, E., Kessler, H., Buchner, J. & Issels, R. D. (2009). Interaction of human heat shock protein 70 with tumor-associated peptides. *Biol. Chem.* **390**, 305–312.
10. Rudiger, S., Germeroth, L., Schneider-Mergener, J. & Bukau, B. (1997). Substrate specificity of the DnaK chaperone determined by screening cellulose-bound peptide libraries. *EMBO J.* **16**, 1501–1507.
11. Gragerov, A. & Gottesman, M. E. (1994). Different peptide binding specificities of hsp70 family members. *J. Mol. Biol.* **241**, 133–135.
12. Hageman, J., van Waarde, M. A., Zylicz, A., Walerych, D. & Kampinga, H. H. (2011). The diverse members of

the mammalian HSP70 machine show distinct chaperone-like activities. *Biochem. J.* **435**, 127–142.
13. Wiech, H., Buchner, J., Zimmermann, M., Zimmermann, R. & Jakob, U. (1993). Hsc70, immunoglobulin heavy chain binding protein, and Hsp90 differ in their ability to stimulate transport of precursor proteins into mammalian microsomes. *J. Biol. Chem.* **268**, 7414–7421.
14. Dudek, J., Greiner, M., Muller, A., Hendershot, L. M., Kopsch, K., Nastainczyk, W. & Zimmermann, R. (2005). ERj1p has a basic role in protein biogenesis at the endoplasmic reticulum. *Nat. Struct. Mol. Biol.* **12**, 1008–1014.
15. Kabani, M., Kelley, S. S., Morrow, M. W., Montgomery, D. L., Sivendran, R., Rose, M. D. *et al.* (2003). Dependence of endoplasmic reticulum-associated degradation on the peptide binding domain and concentration of BiP. *Mol. Biol. Cell*, **14**, 3437–3448.
16. Kassenbrock, C. K., Garcia, P. D., Walter, P. & Kelly, R. B. (1988). Heavy-chain binding protein recognizes aberrant polypeptides translocated in vitro. *Nature*, **333**, 90–93.
17. Davis, D. P., Khurana, R., Meredith, S., Stevens, F. J. & Argon, Y. (1999). Mapping the major interaction between binding protein and Ig light chains to sites within the variable domain. *J. Immunol.* **163**, 3842–3850.
18. Hellman, R., Vanhove, M., Lejeune, A., Stevens, F. J. & Hendershot, L. M. (1999). The in vivo association of BiP with newly synthesized proteins is dependent on the rate and stability of folding and not simply on the presence of sequences that can bind to BiP. *J. Cell Biol.* **144**, 21–30.
19. Nawa, D., Shimada, O., Kawasaki, N., Matsumoto, N. & Yamamoto, K. (2007). Stable interaction of the cargo receptor VIP36 with molecular chaperone BiP. *Glycobiology*, **17**, 913–921.
20. Vanhove, M., Usherwood, Y. K. & Hendershot, L. M. (2001). Unassembled Ig heavy chains do not cycle from BiP in vivo but require light chains to trigger their release. *Immunity*, **15**, 105–114.
21. Haas, I. G. & Wabl, M. (1983). Immunoglobulin heavy chain binding protein. *Nature*, **306**, 387–389.
22. Bole, D. G., Hendershot, L. M. & Kearney, J. F. (1986). Posttranslational association of immunoglobulin heavy chain binding protein with nascent heavy chains in nonsecreting and secreting hybridomas. *J. Cell Biol.* **102**, 1558–1566.
23. Hendershot, L. M. (1990). Immunoglobulin heavy chain and binding protein complexes are dissociated in vivo by light chain addition. *J. Cell Biol.* **111**, 829–837.
24. Meunier, L., Usherwood, Y. K., Chung, K. T. & Hendershot, L. M. (2002). A subset of chaperones and folding enzymes form multiprotein complexes in endoplasmic reticulum to bind nascent proteins. *Mol. Biol. Cell*, **13**, 4456–4469.
25. Feige, M. J., Groscurth, S., Marcinowski, M., Shimizu, Y., Kessler, H., Hendershot, L. M. & Buchner, J. (2009). An unfolded CH1 domain controls the assembly and secretion of IgG antibodies. *Mol. Cell*, **34**, 569–579.
26. Lee, Y. K., Brewer, J. W., Hellman, R. & Hendershot, L. M. (1999). BiP and immunoglobulin light chain cooperate to control the folding of heavy chain and ensure the fidelity of immunoglobulin assembly. *Mol. Biol. Cell*, **10**, 2209–2219.
27. Hendershot, L., Bole, D., Kohler, G. & Kearney, J. F. (1987). Assembly and secretion of heavy chains that do not associate posttranslationally with immunoglobulin heavy chain-binding protein. *J. Cell Biol.* **104**, 761–767.
28. Knarr, G., Gething, M. J., Modrow, S. & Buchner, J. (1995). BiP binding sequences in antibodies. *J. Biol. Chem.* **270**, 27589–27594.
29. Mayer, M., Reinstein, J. & Buchner, J. (2003). Modulation of the ATPase cycle of BiP by peptides and proteins. *J. Mol. Biol.* **330**, 137–144.
30. Zhu, X., Zhao, X., Burkholder, W. F., Gragerov, A., Ogata, C. M., Gottesman, M. E. & Hendrickson, W. A. (1996). Structural analysis of substrate binding by the molecular chaperone DnaK. *Science*, **272**, 1606–1614.
31. Flynn, G. C., Pohl, J., Flocco, M. T. & Rothman, J. E. (1991). Peptide-binding specificity of the molecular chaperone BiP. *Nature*, **353**, 726–730.
32. Marcinowski, M., Holler, M., Feige, M. J., Baerend, D., Lamb, D. C. & Buchner, J. (2011). Substrate discrimination of the chaperone BiP by autonomous and cochaperone-regulated conformational transitions. *Nat. Struct. Mol. Biol.* **18**, 150–158.
33. Huber, R., Deisenhofer, J., Colman, P. M., Matsushima, M. & Palm, W. (1976). Crystallographic structure studies of an IgG molecule and an Fc fragment. *Nature*, **264**, 415–420.
34. Antes, I. (2010). DynaDock: a new molecular dynamics-based algorithm for protein-peptide docking including receptor flexibility. *Proteins*, **78**, 1084–1104.
35. Rudiger, S., Mayer, M. P., Schneider-Mergener, J. & Bukau, B. (2000). Modulation of substrate specificity of the DnaK chaperone by alteration of a hydrophobic arch. *J. Mol. Biol.* **304**, 245–251.
36. Liebscher, M. & Roujeinikova, A. (2009). Allosteric coupling between the lid and interdomain linker in DnaK revealed by inhibitor binding studies. *J. Bacteriol.* **191**, 1456–1462.
37. Pellecchia, M., Montgomery, D. L., Stevens, S. Y., Vander Kooi, C. W., Feng, H. P., Gierasch, L. M. & Zuiderweg, E. R. (2000). Structural insights into substrate binding by the molecular chaperone DnaK. *Nat. Struct. Biol.* **7**, 298–303.
38. Knappe, D., Zahn, M., Sauer, U., Schiffer, G., Strater, N. & Hoffmann, R. (2011). Rational design of oncocin derivatives with superior protease stabilities and antibacterial activities based on the high-resolution structure of the oncocin–DnaK complex. *Chembiochem*, **12**, 874–876.
39. Czihal, P., Knappe, D., Fritsche, S., Zahn, M., Berthold, N., Piantavigna, S. *et al.* (2012). Api88 is a novel antibacterial designer peptide to treat systemic infections with multidrug-resistant gram-negative pathogens. *ACS Chem. Biol.* **7**, 1281–1291.
40. McCarty, J. S., Rudiger, S., Schonfeld, H. J., Schneider-Mergener, J., Nakahigashi, K., Yura, T. & Bukau, B. (1996). Regulatory region C of the *E. coli* heat shock transcription factor, sigma32, constitutes a DnaK binding site and is conserved among eubacteria. *J. Mol. Biol.* **256**, 829–837.

41. Zylicz, M. & Georgopoulos, C. (1984). Purification and properties of the *Escherichia coli* dnaK replication protein. *J. Biol. Chem.* **259**, 8820–8825.
42. Merrifield, R. B. (1965). Solid-phase peptide syntheses. *Endeavour*, **24**, 3–7.
43. Schnolzer, M., Alewood, P., Jones, A., Alewood, D. & Kent, S. B. (1992). In situ neutralization in Boc-chemistry solid phase peptide synthesis. Rapid, high yield assembly of difficult sequences. *Int. J. Pept. Protein Res.* **40**, 180–193.
44. Carpino, L. A. & Han, G. Y. (1970). 9-Fluorenylmethoxycarbonyl function, a new base-sensitive amino-protecting group. *J. Am. Chem. Soc.* **92**, 5748–5749.
45. John, B. & Sali, A. (2003). Comparative protein structure modeling by iterative alignment, model building and model assessment. *Nucleic Acids Res.* **31**, 3982–3992.
46. Sali, A. & Blundell, T. L. (1993). Comparative protein modelling by satisfaction of spatial restraints. *J. Mol. Biol.* **234**, 779–815.